CHAPTER 4

EXPERIMENTAL RESULTS ON A SINGLE-DISK ROTOR

The single-disk rotor described in Chapter 2 and shown in Figure 4.1 was used to evaluate the effectiveness of an AMD in damping subsynchronous vibrations. Two AMDs placed on the rotor offered the capability of being used either to excite the rotor or to perform active control of the rotor, allowing the author to evaluate the effect of the AMD in two locations, at midspan (AMD-13) and at three quarters of the rotor span (AMD-24), without performing any changes in the configuration of the rotor.

Therefore, two sets of experiments were conducted. In the first set, a sine wave was injected through the midspan AMD (AMD-13), while using the AMD at three quarters of the rotor-span (AMD-24) to damp the perturbation. This potentially mimics a turbomachinery scenario where the rotor is excited by an instability mechanism, such as aerodynamic effects at a labyrinth seal, at the midspan location, creating a subsynchronous vibration component. In the second group of experiments, the AMD-24 was used to inject a sine wave while the AMD-13 was used to perform active control on the rotor. This scenario is intended to mimic an excitation due to high-pressure oil seals at quarter-span when the damper is at midspan.

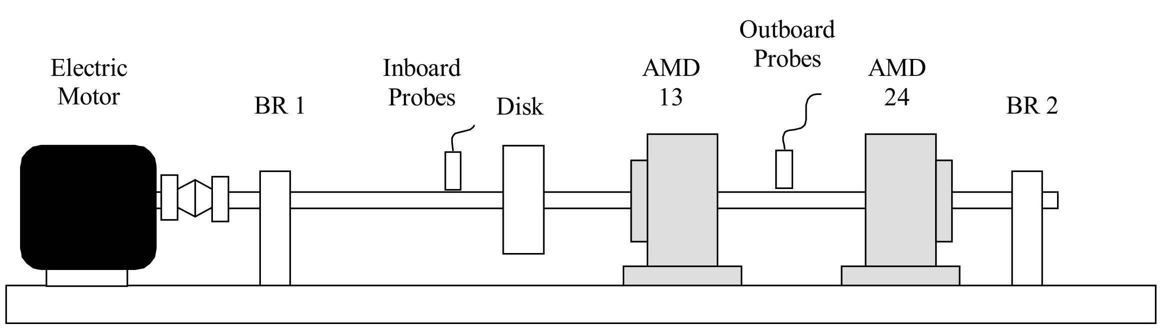

Figure 4.1: Schematic showing the single-disk rotor (not to scale)

Kirk and Miller (1977) mentioned that compressors operating at a speed higher than twice the first critical speed would be likely to exhibit nonsynchronous vibrations. When exhibiting rotordynamic instability a rotor tends to whirl at its natural frequency. The tests were performed running the rotor at approximately twice its first critical speed and injecting a sine wave at approximately the same frequency of its first critical speed.

In addition to an investigation of subsynchronous vibration phenomena, a brief investigation into the effectiveness of an AMD for reducing high frequency supersynchronous vibrations was also conducted. The purpose of this was to examine the potential of an AMD as an actuator for reducing high frequency acoustical noise such as that generated by a gear set. To pursue this objective, a sine wave was injected at 400 Hz. This particular frequency was chosen because it corresponded with a system resonance.

4.1 Case 1: Excitation at Midspan. Damper at three-quarters of the rotor-span (AMD-24)

This scenario is intended to mimic an excitation due to aerodynamic effects at a labyrinth seal, at the midspan location. The results are presented in the following sections.

4.1.1 Excitation at ½ X

The rotor was taken up to 6320 RPM (105 Hz), approximately twice the first critical speed of the rotor configuration with the AMDs off. While the rotor was running at a steady-state speed of 6320 RPM, a 0.75 V sine wave at approximately 3160 RPM (52.7 Hz) was injected through the midspan AMD (AMD-13) resulting in a 2.4 mils pp vibration at this frequency at the vertical inboard probe. The AMD-24 was subsequently turned on resulting in a reduction of this vibration component to 0.7 mils pp. In addition to the 71% reduction of the subsynchronous vibration, the uncompensated synchronous vibration increased from 1.1 mils pp to 1.7 mils pp (55%). The amplitude of the direct vibration decreased from 3.2 mils pp to 2.3 mils pp (28%). The spectra of the uncompensated vibration signal at the vertical inboard probe with the AMD-24 “off” and “on” are shown in Figure 4.2 (a) and (b), respectively. Table 4.1 lists the variation in amplitude of the synchronous, subsynchronous and direct vibrations at the four probe locations. For this case, the stiffness expected for the AMD-24 is 1450 lbf/in at 105 Hz and 1285 lbf/in at 52.7 Hz. The expected damping for the AMD-24 is 2.95 lb-s/in at both frequencies.

After observing that the quarter-span AMD (AMD-24) was able to reduce the amplitude of the ½ X subsynchronous and direct vibrations when the rotor kit was running at 6320 RPM (105 Hz), the rotor kit was taken up to 8160 RPM (136 Hz), twice the first critical speed of the rotor configuration when the AMD-24 is on acting as a third bearing, shown in Figure 2.9. A sine wave at 4080 RPM (68 Hz) was injected through the AMD-13 resulting in a 0.7 mils pp vibration at this frequency at the vertical inboard probe. The AMD-24 was subsequently turned on resulting in no variation in the amplitude of the subsynchronous (68 Hz) vibration. The amplitude of the uncompensated synchronous vibration increased from 0.9 mils pp to 1.5 mils pp (67%) and the amplitude of the direct vibration increased from 1.5 mils pp to 2.2 mils pp (47%). Figures 4.3 (a) and (b) show the spectra of the uncompensated vibration signal at the vertical inboard probe with the AMD-24 “off” and “on” respectively, and Table 4.2 lists the variation in amplitude of the synchronous, subsynchronous and direct vibrations at the four probe locations. For this case, the stiffness expected for the AMD-24 is 1593 lbf/in at 136 Hz and 1322 lbf/in at 52.7 Hz. The expected damping for the AMD-24 is 2.95 lb-s/in at 136 Hz. and 2.94 lb-s/in at 52.7 Hz.

Even though the reason of the increase of the uncompensated synchronous vibration is not completely clear, it may be attributed to the fact that the damping provided by the AMD is about constant with respect to the frequency while the stiffness increases with the frequency. Since this test was performed at a higher frequency, if compared with the previous test, there might be a decrease in the effective damping of the AMD due to an increase in the rotational speed.

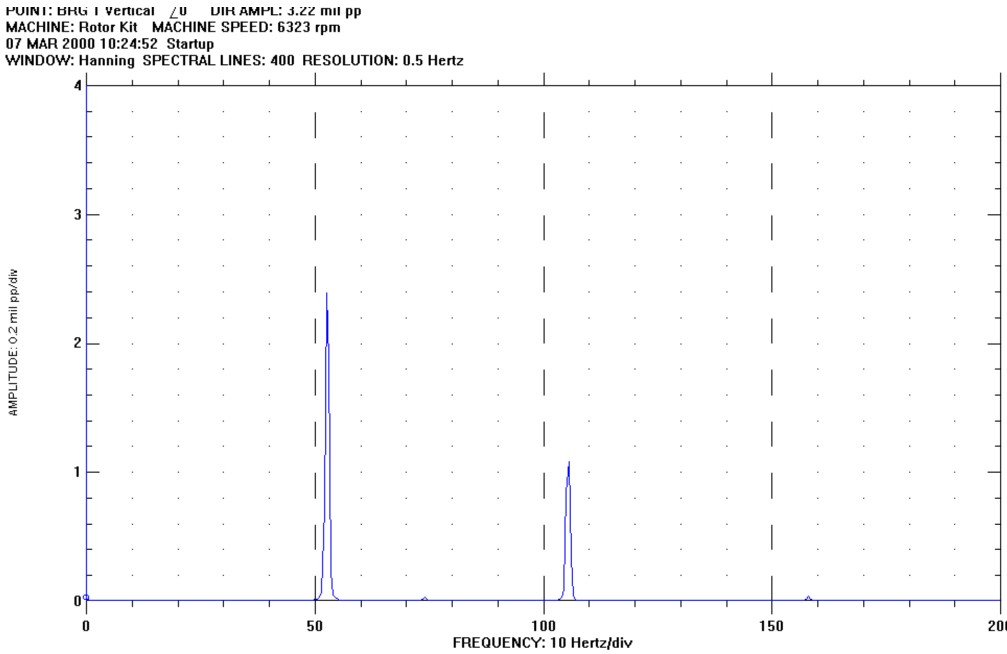

(a)

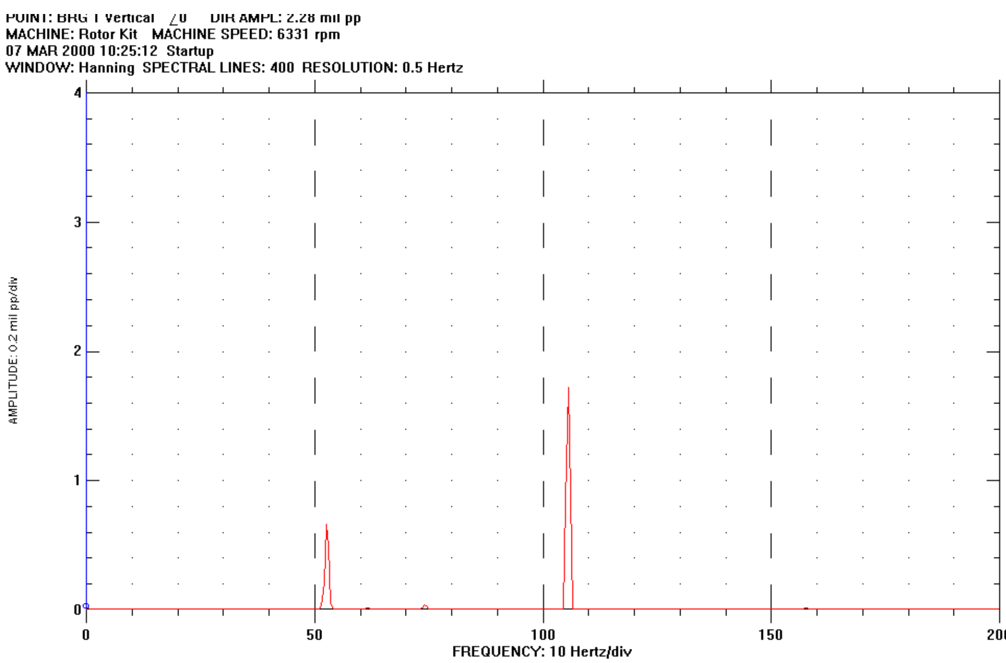

(b)

Figure 4.2: Spectrum of the vibration signal at the vertical inboard probe, single-disk rotor at 6320 RPM (105 Hz) and a perturbation at 52.7 Hz through AMD-13. (a) AMD-24 off. (b) AMD-24 on.

Table 4.1: Effect of the AMD-24 on the direct, synchronous and subsynchronous amplitudes of the single-disk rotor at 6320 RPM (105 Hz) with a perturbation of 0.75 V at 52.7 Hz, ½ X the rotational speed, through the AMD-13.

Probe Location	**AMD-24 "Off"**			**AMD-24 "On"**			**Variation in Amplitude**		
	Direct Amplitude mils pp	Synchronous Amplitude mils pp	Subsynchronous Amplitude mils pp	Direct Amplitude mils pp	Synchronous Amplitude mils pp	Subsynchronous Amplitude mils pp	Direct Amplitude %	Synchronous Amplitude %	Subsynchronous Amplitude %
Inboard vertical	3.2	1.1	2.4	2.3	1.7	0.7	-28	+55	-71
Inboard horizontal	3.4	1.1	2.4	2.4	1.8	0.7	-29	+64	-71
Outboard vertical	5.4	2.9	3.4	3.9	3.2	0.8	-28	+10	-76
Outboard horizontal	4.8	2.7	2.5	3.4	2.9	0.6	-29	+7	-76

4.1.2 Excitation at 1/3 X

For this test, the rotor was taken up to 6320 RPM (105 Hz) and a 0.75 V sine wave at 2100 RPM (35 Hz), simulating a 1/3 X subsynchronous vibration, was injected through the midspan AMD-13, resulting in a 0.7 mils pp vibration at this frequency at the vertical inboard probe. The AMD-24 was subsequently turned on resulting in a reduction of this vibration component to 0.4 mils pp. Figures 4.4 (a) and (b) show the spectra of the uncompensated vibration signal at the vertical inboard probe with the AMD-24 "off" and "on" respectively. In addition to the 43% reduction in subsynchronous vibration, the uncompensated synchronous vibration increased 58%, from 1.2 mils pp to 1.9 mils pp, and the amplitude of the direct vibration increased 10 %, from 2.0 mils pp to 2.2 mils pp. Table 4.3 lists the variation in the amplitude of the synchronous, subsynchronous and direct vibrations at the four probe locations. For this case, the stiffness expected for the AMD-24 is 1450 lbf/in at 105 Hz and 1255 lbf/in at 35 Hz. The expected damping for the AMD-24 is 2.95 lb-s/in at 105 Hz and 2.93 lb-s/in at 35 Hz.

4.1.3 Excitation at 400 Hz

For this test, the rotor was taken up to 6320 RPM (105 Hz) and a 2.0 V sine wave at 400 Hz, which corresponds with a resonance of the system, was injected through the midspan AMD-13, resulting in a 0.2 mils pp vibration at this frequency at the vertical inboard probe. Obtaining bigger amplitudes at 400 Hz was not possible as the AMD system became unstable when a voltage higher than 2.0 V was injected. The AMD-24 was subsequently turned on resulting in a reduction of this vibration component to 0.1 mils pp. Figures 4.5 (a) and (b) show the spectra of the vibration signal at the vertical inboard probe with the AMD-24 "off" and "on" respectively. In addition to the 50% reduction in supersynchronous vibration, the uncompensated synchronous vibration increased 42%, from 1.2 mils pp to 1.7 mils pp, and the amplitude of the direct vibration increased 27 %, from 1.5 mils pp to 1.9 mils pp. Table 4.4 lists the variation in the amplitude of the synchronous, supersynchronous and direct vibrations at the four probe locations. Even though a pattern in reduction of the supersynchronous vibration was observed, these results have to be carefully reviewed, since the amplitude of the subsynchronous vibrations is very small and is close to the uncertainty of the measurements. For this case, the stiffness expected for the AMD-24 is 1593 lbf/in at 105 Hz and 1322 lbf/in at 35 Hz. The expected damping for the AMD-24 is 2.95 lb-s/in at 105 Hz and 2.94 lb-s/in at 35Hz

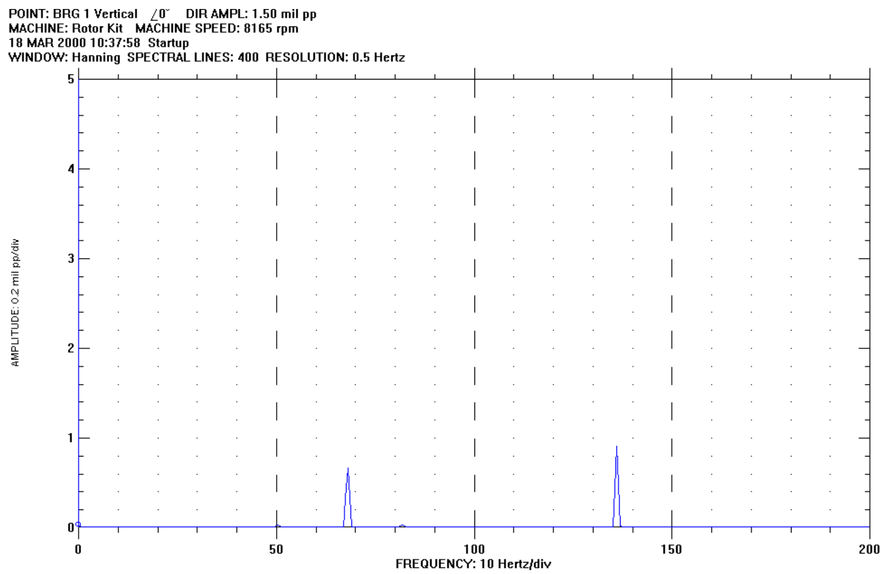

(a)

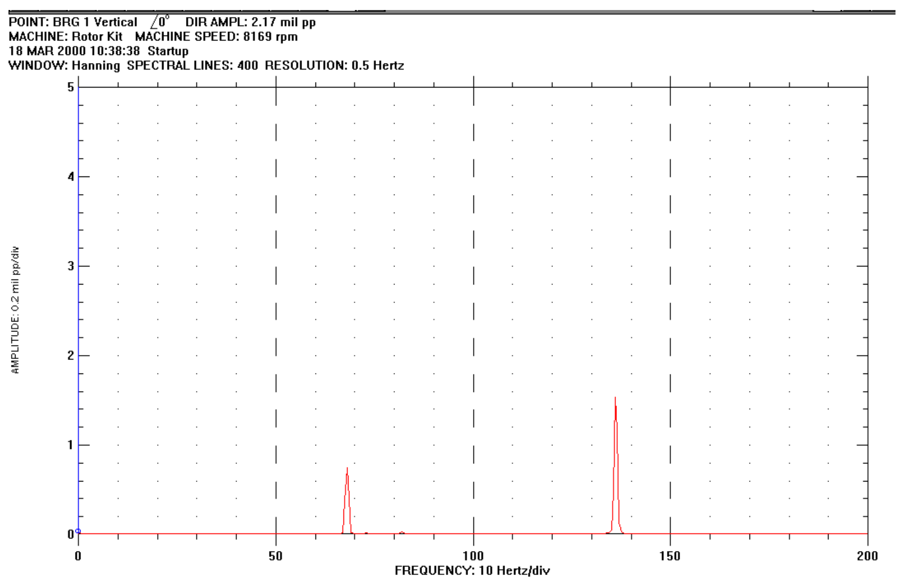

(b)

Figure 4.3: Spectrum of the vibration signal at the vertical inboard probe, single-disk rotor running at 8160 RPM (136 Hz) and a perturbation at 68 Hz through AMD-13. (a) AMD-24 off. (b) AMD-24 on.

Table 4.2: Effect of the AMD-24 on the direct, synchronous and subsynchronous amplitudes of the single-disk rotor at 8160 RPM (136 Hz) with a perturbation of 0.75 V at 68 Hz, ½ X the rotational speed, through AMD-13.

Probe Location	**AMD-24 "Off"**			**AMD-24 "On"**			**Variation in Amplitude**		
	Direct Amplitude mils pp	Synchronous Amplitude mils pp	Subsynchronous Amplitude mils pp	Direct Amplitude mils pp	Synchronous Amplitude mils pp	Subsynchronous Amplitude mils pp	Direct Amplitude %	Synchronous Amplitude %	Subsynchronous Amplitude %
Inboard vertical	1.5	0.9	0.7	2.2	1.5	0.7	+ 47	+ 67	0
Inboard horizontal	1.5	0.8	0.7	2.6	1.7	1.2	+ 73	+ 113	+ 71
Outboard vertical	4.9	4.1	0.9	4.4	3.5	0.9	- 10	- 15	0
Outboard horizontal	4.5	3.9	0.7	4.4	3.4	1.0	- 2	- 13	- 43

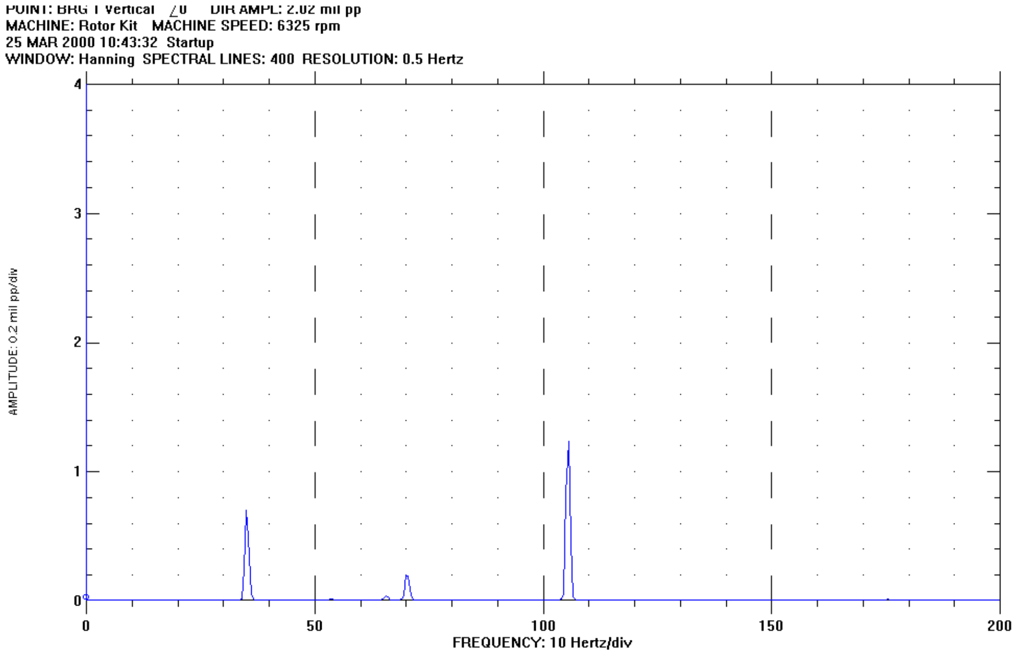

(a)

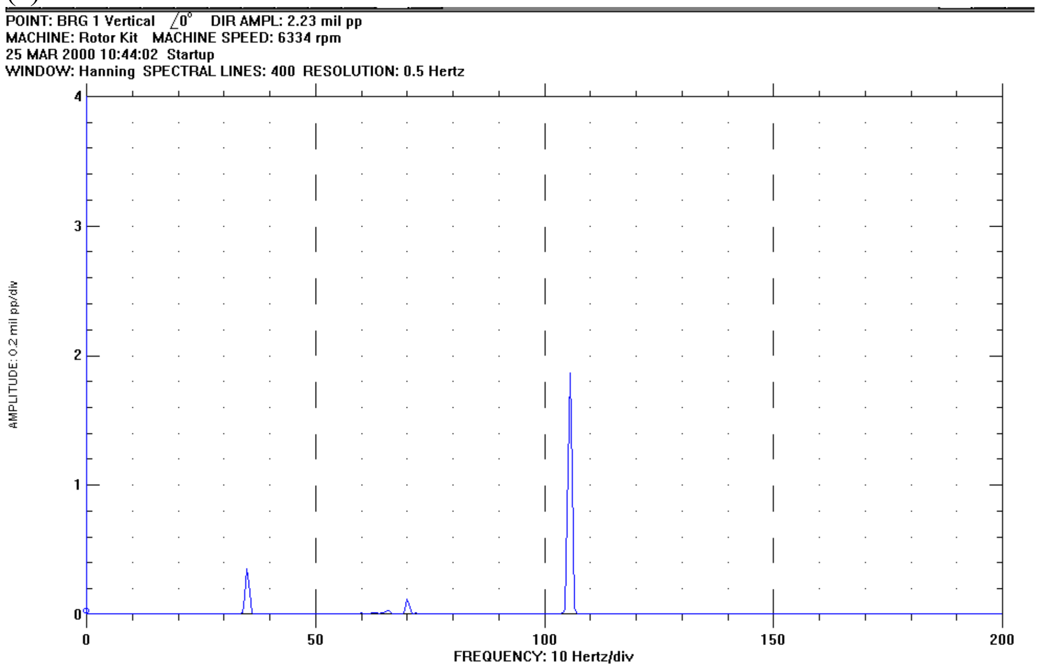

(b)

Figure 4.4 Spectrum of the vibration signal at the vertical inboard probe, single-disk rotor at 6320 RPM (105 Hz) and a perturbation at 35 Hz through AMD-13. (a) AMD-24 off. (b) AMD-24 on.

Table 4.3 Effect of the AMD-24 on the direct, synchronous and subsynchronous amplitudes of the single-disk rotor at 6320 RPM (105 Hz) with a perturbation of 0.75 V at 35 Hz, 1/3 X the rotational speed, through the AMD-13

Probe Location	**AMD-24 "Off"**			**AMD-24 "On"**			**Variation in Amplitude**		
	Direct Amplitude mils pp	Synchronous Amplitude mils pp	Subsynchronous Amplitude mils pp	Direct Amplitude mils pp	Synchronous Amplitude mils pp	Subsynchronous Amplitude mils pp	Direct Amplitude %	Synchronous Amplitude %	Subsynchronous Amplitude %
Inboard vertical	2.0	1.2	0.7	2.2	1.9	0.4	+ 10	+ 58	- 43
Inboard horizontal	2.2	1.4	0.9	2.5	2.0	0.4	+ 14	+ 43	- 56
Outboard vertical	4.6	3.4	1.0	3.9	3.4	0.5	- 15	0	- 50
Outboard horizontal	4.0	3.1	1.0	3.5	3.1	0.4	- 13	0	- 60

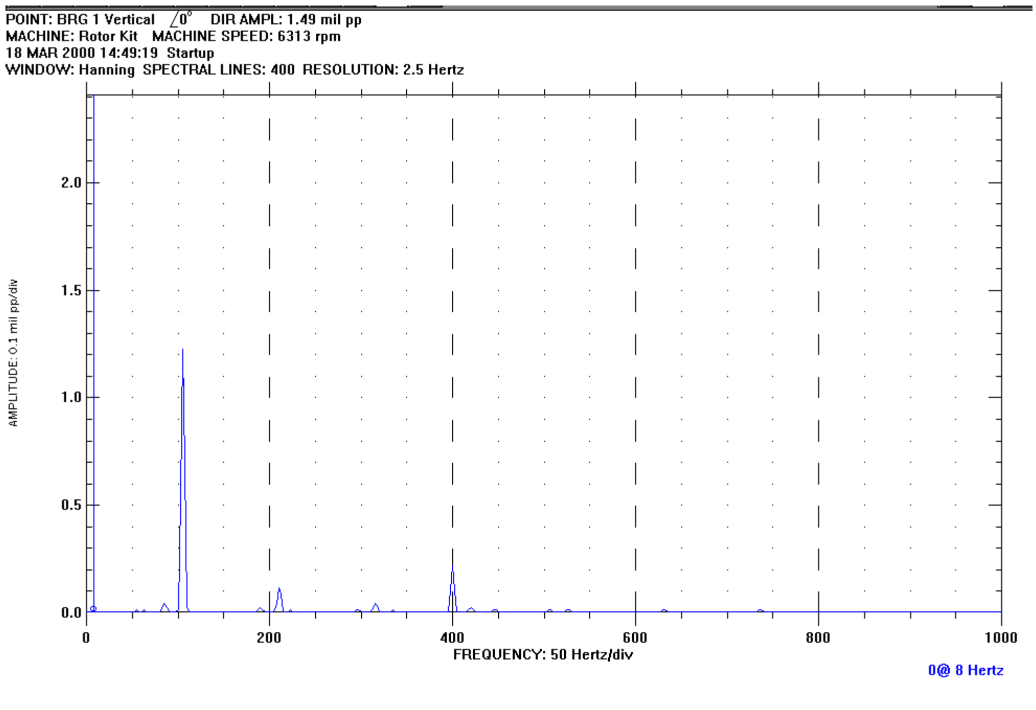

(a)

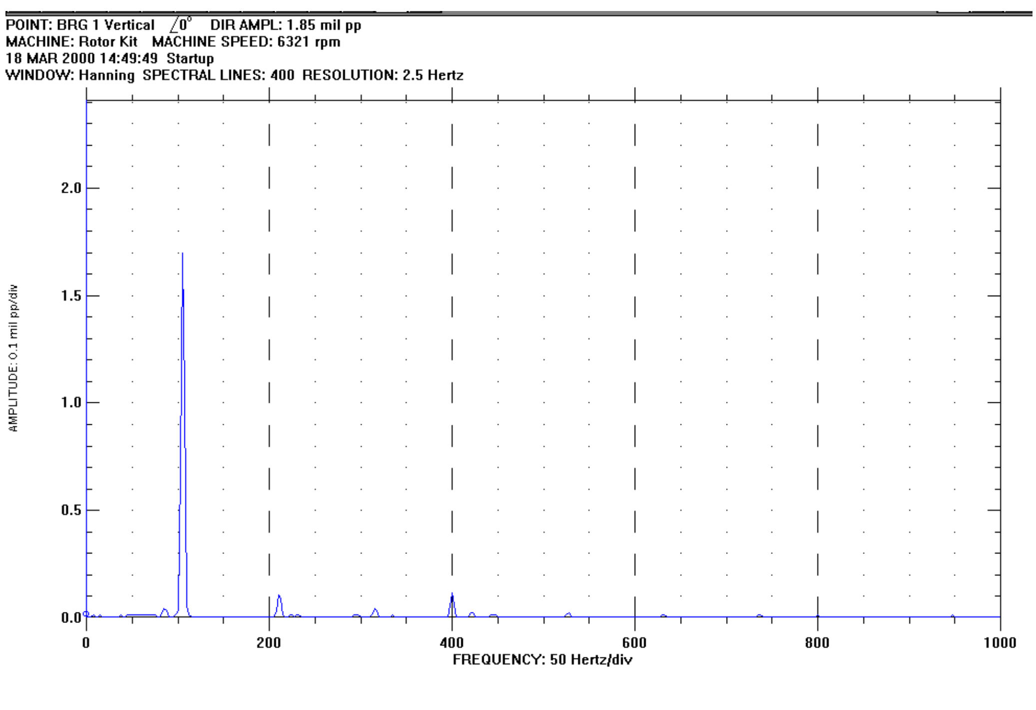

(b)

Figure 4.5: Spectrum of the vibration signal at the vertical inboard probe, rotor running at 105 Hz and a perturbation at 400 Hz through AMD-13. (a) AMD-24 off. (b) AMD-24 on

Table 4.4 Effect of the AMD-24 on the direct, synchronous and supersynchronous amplitudes of the single-disk rotor at 6320 RPM (105 Hz) with a perturbation of 2.0 V at 400 Hz, through the AMD-13

Probe Location	**AMD-24 "Off"**			**AMD-24 "On"**			**Variation in Amplitude**		
	Direct Amplitude mils pp	Synchronous Amplitude mils pp	Supersynchronous Amplitude mils pp	Direct Amplitude mils pp	Synchronous Amplitude mils pp	Supersynchronous Amplitude mils pp	Direct Amplitude %	Synchronous Amplitude %	Supersynchronous Amplitude %
Inboard vertical	1.5	1.2	0.2	1.9	1.7	0.1	+ 27	+ 42	- 50
Inboard horizontal	1.6	1.2	0.3	2.0	1.8	0.1	+ 25	+ 50	- 67
Outboard vertical	3.5	3.2	0.1	3.5	3.2	0.1	0	0	0
Outboard horizontal	3.2	2.9	0.2	3.1	2.9	0.2	- 3	0	0

4.2 Case 2: Excitation at three quarters of rotor-span
Damper at midspan (AMD-13)

This scenario is intended to mimic an excitation due to high-pressure oil seals at quarter-span when the damper is at midspan. The results are presented in the following sections.

4.2.1 Excitation at ½ X

In this investigation, the rotor was taken up to 6320 RPM (105 Hz), twice the first critical speed of the rotor configuration with the AMDs off and a 1.0 V sine wave at 3160 RPM (52.7 Hz) was injected through the AMD-24 resulting in 1.4 mils pp vibration at that frequency at the vertical inboard probe. The AMD-13 was subsequently turned on resulting in a reduction of this vibration component to 0.1 mils pp. In addition to the 93% reduction of the subsynchronous vibration, the uncompensated synchronous vibration increased from 1.1 mils pp to 3.5 mils pp (218%). The amplitude of the direct vibration increased as well, from 2.4 mils pp to 4.2 mils pp (75%).

The addition of the AMD-13 increases the stiffness and the damping of the system. Even though the damping increases as a result of the addition of the AMD, the more significant contribution to the reduction of the subsynchronous response is due to an increase of the stiffness, which increases the natural frequency of the system from 2920 RPM, 305 rad/s to 5120 RPM, 536 rad/s. The same effect increases the amplitude of the synchronous vibration.

The spectra of the uncompensated vibration signal at the vertical inboard probe with the AMD-13 "off" and "on" are shown in Figure 4.6 (a) and (b), respectively. The variations in amplitude of the synchronous, subsynchronous and direct vibrations at the four probe locations are listed in Table 4.5. For this case, the stiffness expected for the AMD-13 is 1450 lbf/in at 105 Hz and 1285 lbf/in at 52.7 Hz. The expected damping for the AMD-24 is 2.95 lb-s/in at both frequencies.

These results suggest that the AMD-13 is very effective in damping subsynchronous vibrations (with maximum amplitudes at the midspan) but produces a change in the dynamics of the rotor in such a way that it is not only ineffective but also harmful with respect to synchronous vibrations.

4.2.2 Excitation at 1/3 X

In the present test, the rotor was taken up to 6320 RPM (105 Hz) and a 1.0 V sine wave at 2100 RPM (35 Hz), simulating a 1/3 X subsynchronous vibration, was injected through the AMD-24 resulting in a 0.4 mils pp at that frequency at the vertical inboard probe. The AMD-24 was subsequently turned on resulting in a reduction of this vibration component to 0.1 mils pp. In addition to the 75% reduction in subsynchronous vibration, the uncompensated synchronous vibration increased from 1.3 mils pp to 4.3 mils pp (231%). The amplitude of the direct vibration increased as well, from 1.7 mils pp to 4.4 mils pp (159%). Figures 4.7 (a) and (b) show the spectra of the uncompensated vibration signal at the vertical inboard probe before and after the AMD-13 was turned "on" respectively. Table 4.6 lists the variation in the amplitude of the synchronous, subsynchronous and direct vibrations at the four probe locations. For this case, the stiffness expected for the AMD-24 is 1450 lbf/in at 105 Hz and 1255 lbf/in at 35 Hz. The expected damping for the AMD-24 is 2.95 lb-s/in at 105 Hz and 2.93 lb-s/in at 35 Hz.

Even though a pattern in reduction of the 1/3 X subsynchronous vibration was observed, these results have to be carefully reviewed, since the amplitude of the subsynchronous vibrations is very small and is close to the uncertainty of the measurements.

When the AMD-13 is turned on, it adds stiffness to the system changing the location of the first critical speed, from 2920 RPM (48.7 Hz) to 5120 RPM (85.3 Hz), resulting in an increase of the uncompensated synchronous vibration.

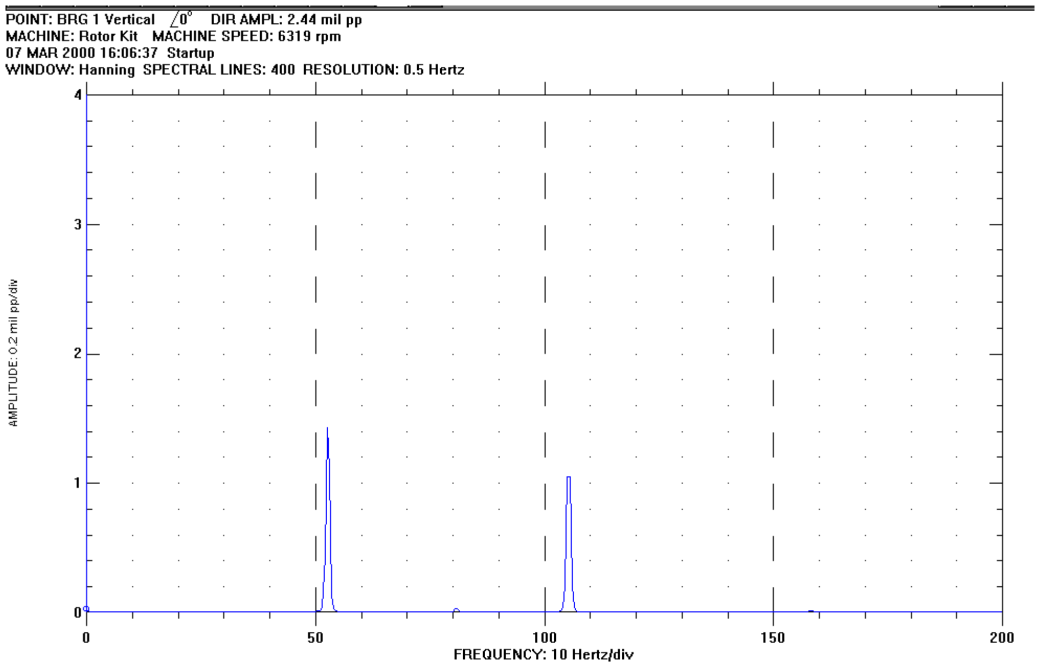

(a)

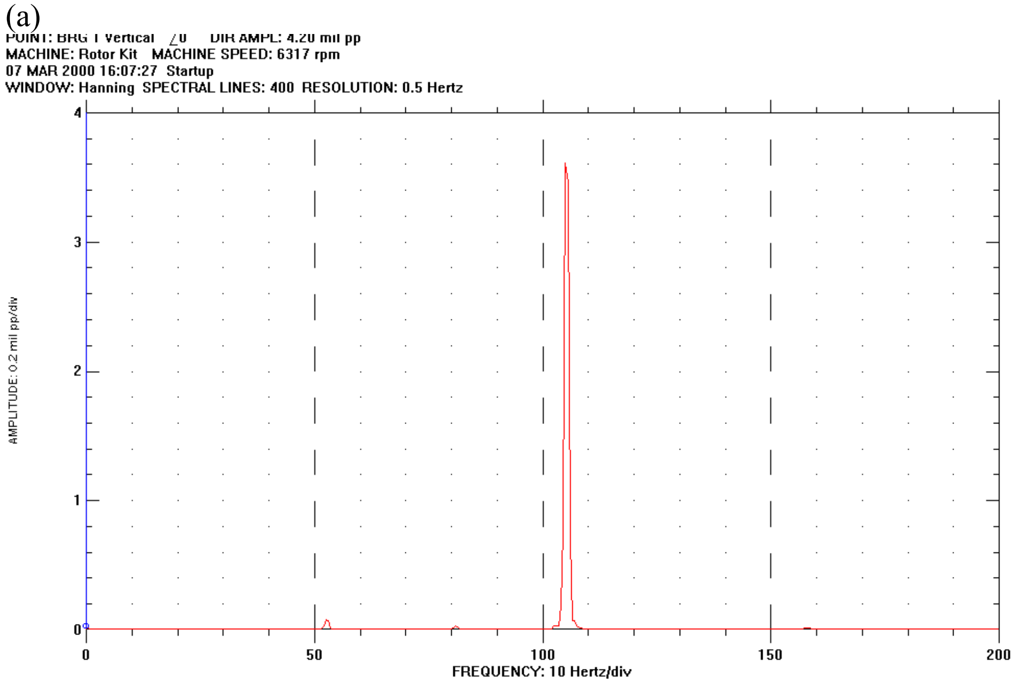

(b)

Figure 4.6: Spectrum of the vibration signal at the vertical inboard probe, single-disk rotor at 6320 RPM (105 Hz) and a perturbation at 52.7 Hz through AMD-24. (a) AMD-13 off. (b) AMD-13 on.

Table 4.5: Effect of the AMD-13 on the direct, synchronous and subsynchronous amplitudes of the single-disk rotor at 6320 RPM (105 Hz) with a perturbation of 1.0 V at 52.7, ½ X the rotational speed, through AMD-24

Probe Location	**AMD-13 "Off"**			**AMD-13 "On"**			**Variation in Amplitude**		
	Direct Amplitude mils pp	Synchronous Amplitude mils pp	Subsynchronous Amplitude mils pp	Direct Amplitude mils pp	Synchronous Amplitude mils pp	Subsynchronous Amplitude mils pp	Direct Amplitude %	Synchronous Amplitude %	Subsynchronous Amplitude %
Inboard vertical	2.4	1.1	1.4	4.2	3.5	0.1	+ 75	+ 218	- 93
Inboard horizontal	2.3	1.1	1.3	3.7	2.9	0.1	+ 61	+ 155	- 92
Outboard vertical	5.0	2.7	2.0	4.4	3.5	0.2	- 12	+ 44	- 90
Outboard horizontal	3.8	2.5	1.4	3.1	2.4	0.2	- 18	- 4	- 86

Table 4.6: Effect of the AMD-13 on the direct, synchronous and subsynchronous amplitudes of the single-disk rotor at 6320 RPM (105 Hz) with a perturbation of 0.75 V at 35 Hz, 1/3 X the rotational speed, through AMD-24

Probe Location	**AMD-13 "Off"**			**AMD-13 "On"**			**Variation in Amplitude**		
	Direct Amplitude mils pp	Synchronous Amplitude mils pp	Subsynchronous Amplitude mils pp	Direct Amplitude mils pp	Synchronous Amplitude mils pp	Subsynchronous Amplitude mils pp	Direct Amplitude %	Synchronous Amplitude %	Subsynchronous Amplitude %
Inboard vertical	1.7	1.3	0.4	4.4	4.3	0.1	+ 159	+ 231	- 75
Inboard horizontal	1.8	1.4	0.5	3.8	3.6	0.1	+ 111	+ 157	- 80
Outboard vertical	4.2	3.5	0.6	4.8	4.5	0.2	+ 14	+ 29	- 67
Outboard horizontal	3.7	3.1	0.6	3.2	3.0	0.2	- 14	- 3	- 67

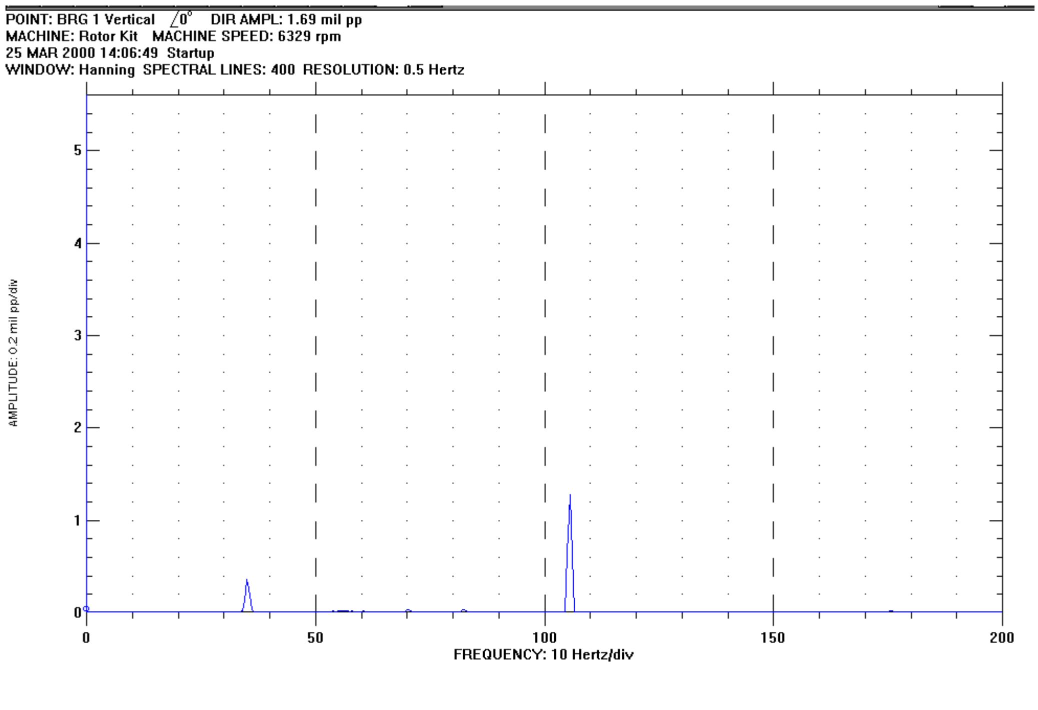

(a)

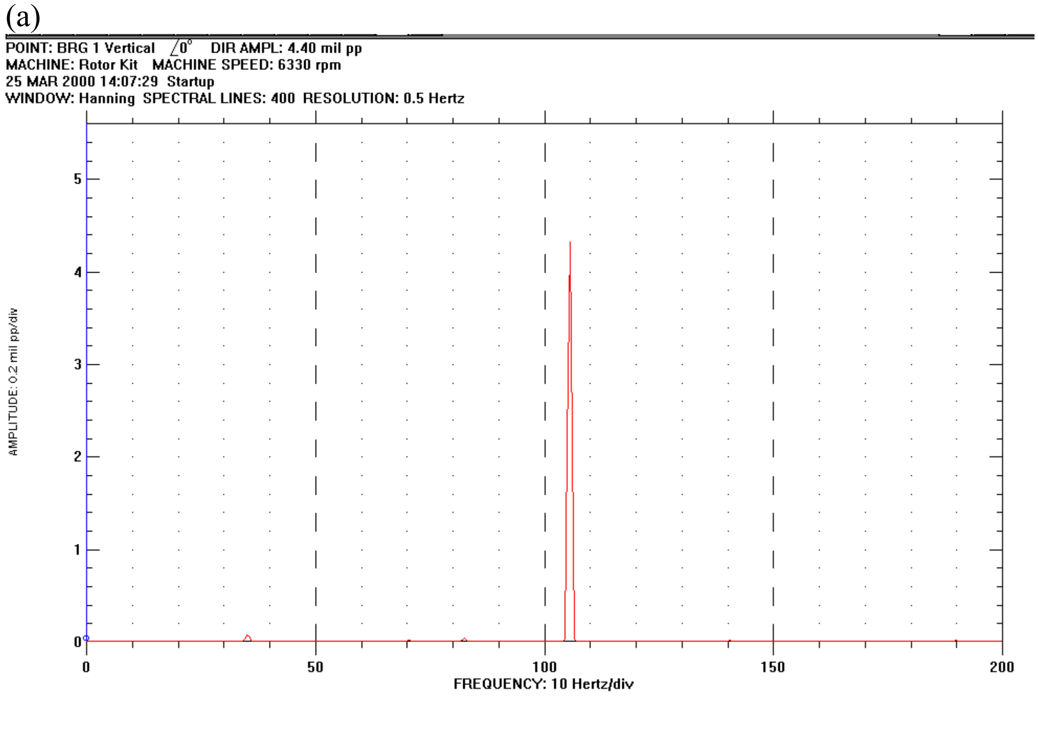

(b)

Figure 4.7: Spectrum of the vibration signal at the vertical inboard probe, single-disk rotor at 6320 RPM (105 Hz) and a perturbation at 35 Hz through AMD-24. (a) AMD-13 off. (b) AMD-13 on